Coping with the climate: Cuticular hydrocarbon acclimation of ants under constant and fluctuating conditions

Philipp P. Sprenger[1*], Lars H. Burkert[1], Bérengère Abou[2], Walter Federle[3], Florian Menzel[1]

[1] Institute of Organismic and Molecular Evolution, Faculty of Biology, Johannes Gutenberg University, Mainz, Germany

[2] Matière et Systèmes Complexes (MSC), UMR CNRS 7057, Université Paris Diderot, Paris, France

[3] Department of Zoology, University of Cambridge, Cambridge, United Kingdom

[*] Corresponding author: phspreng@uni-mainz.de

Running headline:

Ant cuticular hydrocarbon acclimation

Summary statement:

Ants adjust their cuticular hydrocarbon layer to humidity and temperature, thereby maintaining its functionality for waterproofing and communication. Varying and constant temperature regimes had different effects on hydrocarbon composition.

Abstract

Terrestrial arthropods achieve waterproofing by a layer of cuticular hydrocarbons (CHCs). At the same time, CHCs also serve as communication signals. To maintain waterproofing under different climate conditions, insects adjust the chemical composition of their CHC layer, but this may affect the communication via CHC. The detailed acclimatory changes of CHCs and how these influence their physical properties are still unknown. Here, we studied acclimation in two closely related ant species with distinct CHC profiles, *Myrmica rubra* and *Myrmica ruginodis*, in response to constant or fluctuating temperature and humidity regimes. We measured how acclimation affected CHC composition and viscosity, and the ants' drought survival. In both species, CHC composition showed strong, predictable responses to temperature regimes. Warm-acclimated individuals had higher proportions of linear alkanes, and less methyl-branched or unsaturated CHCs. These changes coincided with higher solid content and viscosity of CHCs in warm-acclimated ants. Temperature fluctuation caused effects similar to constant-cool conditions in *M. rubra*, but led to entirely different profiles in *M. ruginodis*, suggesting that fluctuating and constant conditions pose very different challenges. Acclimation to dry conditions led to higher absolute amounts of CHCs, which increased the ants' drought survival, whereas temperature acclimation did not. Hence, the temperature-induced CHC changes cannot be explained by the need for waterproofing alone. While these changes could be non-adaptive, we propose that they serve to maintain a constant CHC viscosity, which may be essential for communication and other functions.

Key words

Cuticular hydrocarbon acclimation, desiccation resistance, drought survival, phenotypic plasticity, microrheology, viscosity

Introduction

Climate change is predicted to raise the global mean temperature, increase temperature fluctuations, make weather events such as heat waves or drought events more common, and change the global distribution of water availability and precipitation (Coumou and Rahmstorf, 2012; Fung et al., 2011). Therefore, the effects of climatic factors such as temperature and humidity on animals have attracted increasing scientific interest. As a short-term mechanism to cope with altered conditions, animals can acclimate to climate conditions by modifying their behaviour, morphology and physiology via phenotypic plasticity (Angilletta Jr., 2009). Phenotypic plasticity of physiological traits can increase the resistance of ectothermic animals to climate change (Seebacher et al., 2015).

Acclimation to different temperatures has been shown for a variety of animals (Angilletta Jr., 2009), but responses differ between constant and fluctuating temperatures (Colinet et al., 2015). In addition to temperature, humidity and its interaction with temperature may affect the fitness of ectothermic animals (Chown et al., 2011; Terblanche and Kleynhans, 2009). Terrestrial arthropods should be highly susceptible to climatic changes, as their metabolic rate is directly affected by the environmental temperature and their large surface-to-volume ratio makes them vulnerable to water loss. Most water loss under ambient temperatures occurs through the cuticle (Edney, 1977; Hadley, 1994). Therefore, it is important to understand the mechanisms insects use to reduce cuticular water loss.

In insects, waterproofing is achieved by a hydrocarbon layer on the cuticle (Blomquist and Bagnères, 2010). Cuticular hydrocarbons (CHC) comprise a complex mixture of *n*-alkanes, methyl-branched alkanes and unsaturated hydrocarbons (alkenes) (Blomquist, 2010). These compounds differ in the carbon chain length and the number of methyl groups and/or double bonds. In addition to waterproofing, CHCs also serve several other functions, most importantly as communication signals in many insect species (Blomquist and Bagnères,

2010). Especially in social insects, cuticular hydrocarbons encode a plethora of information, regulating (amongst other things) nestmate recognition and the division of labour within a colony (Leonhardt et al., 2016). For example, behavioural castes among ant workers (such as scouts, foragers and nurses) possess quantitatively different CHC profiles, which can trigger different behavioural responses in their nestmates (Greene and Gordon, 2003; Pamminger et al., 2014; Wagner et al., 2001).

Variation in cuticular waterproofing depends both on the absolute amount and quantitative composition of the CHC layer (Chown et al., 2011; Edney, 1977). The strong temperature dependence of the waterproofing function of insect cuticle is thought to be caused by a 'melting' of the CHCs, which is influenced by their chemical composition (Gibbs, 1998; Gibbs and Pomonis, 1995). Early studies on several insect species showed that evaporation of water through a CHC layer increases drastically if the ambient temperature is raised above a critical temperature T_c (Beament, 1945; Beament, 1958; Beament, 1959; Gibbs, 2002; Ramsay, 1935; Rourke and Gibbs, 1999; Wigglesworth, 1945). The melting point of the CHC layer increases when CHC molecules align and aggregate. Generally, *n*-alkane molecules aggregate most tightly due to van der Waals forces, and this aggregation increases with chain length. Hydrocarbons with strong van der Waals bonds (e.g. *n*-alkanes, monomethyl alkanes) can even crystallize (Brooks et al., 2015). Thus, *n*-alkanes should provide the best waterproofing to the insect, especially so if they have high chain lengths. In contrast, methyl groups and double bonds disrupt the linear geometry of *n*-alkanes and therefore hinder a tight molecular aggregation. The melting temperature T_m of a hydrocarbon therefore decreases from *n*-alkanes to monomethyl alkanes, dimethyl alkanes, alkenes, and alkadienes (in this order) (Gibbs, 1998; Gibbs and Pomonis, 1995). However, hydrocarbon mixtures do not have a sharp melting point. Rather, melting occurs over a wider temperature range (Gibbs, 1995). Moreover, tight molecular cohesion of cuticular hydrocarbons may not only increase their

melting point, but also increase their viscosity. The higher the viscosity of the CHC layer, the lower is the diffusion rate of CHC molecules across the body surface (the diffusion coefficient is inversely proportional to viscosity according to the Stokes-Einstein relation, Einstein, 1905). However, the ability of CHC molecules to move across the cuticle is essential for many biological functions. For example, CHCs can only serve as communication signals if they are sufficiently liquid to diffuse and spread across the cuticle, or onto sensory sensilla of other insects that act as communication partners (Blomquist and Bagnères, 2010; Maitani et al., 2010). Low CHC viscosity may also be essential for the repair of scratches (Wigglesworth, 1945), for the lubrication of joints (Cooper et al., 2009; Gorb, 2001) and for the rapid attachment and detachment of sticky footpads (Labonte and Federle, 2015). Hence, improving waterproofing via the production of CHCs with a tighter molecular cohesion and higher melting points may increase CHC viscosity and thereby compromise several other functions of the CHC layer. Nevertheless, previous studies on arthropod CHC have not considered CHC viscosity and the potential trade-offs of waterproofing with other functions. As a first step, in this study we have quantified CHC viscosity by using microrheology, a technique that allows measurements for extremely small volumes of material (~30 picolitres). Since molecular aggregation and viscosity depend on temperature, these physical effects should matter for an insect that experiences fluctuations of environmental temperature and/or humidity over time. Indeed, insects can adjust their CHC profile to climatic conditions (Gibbs and Mousseau, 1994; Hadley, 1977). Notably, it has been reported that physiological acclimation can differ between constant and fluctuating temperatures, e.g. in the expression of heat shock proteins and immune activity (Fischer et al., 2011) or fatty acid composition (van Dooremalen et al., 2011). Probably because of the nonlinear relationship between temperature and metabolic processes, fluctuating temperatures can lead to effects which differ from those reached at constant temperatures (Colinet et al., 2015).

Cuticular hydrocarbon profiles of insects differ considerably within and between species. Even closely related species often possess entirely different CHC profiles, which may not only differ in their waterproofing function and viscosity at a given (constant) temperature, but also in their ability to function across a temperature range with daily fluctuations. Little is still known about how insects adjust their CHC profile to constant vs. fluctuating climate regimes, and how the different hydrocarbon classes contribute to waterproofing. In particular, it is unknown whether species with different abundance of unsaturated and methyl-branched hydrocarbons can acclimate to the same extent, and survive challenging environmental conditions.

Here, we measured acclimatory CHC changes and survival of acclimated workers in two closely related ant species with strongly different CHC profiles, as well as the concomitant changes in CHC viscosity. Alkadienes dominate the profile of *Myrmica ruginodis* NYLANDER 1846, but are absent in its sister species *Myrmica rubra* (LINNAEUS 1758), whose profile is rich in di-, tri- and tetramethyl alkanes (Fig. 1). The latter substances, in turn, are rare or absent in *M. ruginodis*. This reflects two frequent CHC types in ants, where species either possess multi-methyl alkanes or unsaturated compounds, but rarely both substance classes in higher quantities (Menzel et al., 2017). The CHC profile may reflect different climatic niches (Menzel et al., 2017), with *M. ruginodis* inhabiting cooler and/or damper habitats than *M. rubra*, and representing the *Myrmica* species most adapted to cool temperatures among all old-world species (Radchenko and Elmes, 2010). However, *M. ruginodis* and *M. rubra* are ecologically similar and frequently co-occur in the same sites.

We expected that, at higher temperatures, both species produce CHC profiles with more saturated and unbranched hydrocarbon classes to enhance waterproofing. Because of the division of labour in ants, workers foraging outside the nest should need stronger protection against environmental conditions than nurses, which remain inside. By disentangling

temperature and humidity acclimation, we compared the effects of both factors on CHC composition and ant survival. Lastly, we used microrheology as a novel tool to quantify the viscosity of CHC profiles of ants acclimated to different temperatures.

Materials and Methods

STUDY ORGANISMS

Both of our study species, *M. rubra* and *M. ruginodis* are widely distributed across Europe, have similar life-histories and can be found in the same habitats (Radchenko and Elmes, 2010). We collected 15 colonies of each species in the region around Freiburg (Germany) in April and June 2015. Colonies were collected at the following specific locations: Vogelsangpass (48.087 N, 7.697 E – both species), Eichelspitze (48.090 N, 7.694 E – *M. ruginodis* only), Burkheim/Rheinauen (48.099 N, 7.582 E – both species), Mooswald/Opfinger See (48.004 N, 7.752 E – *M. ruginodis* only) and Eichberg (47.975 N, 7.893 E – *M. rubra* only). They were kept in their original nesting material in plastic boxes (235 x 175 x 90 mm, Lifeca GmbH & Co. KG, Bad Salzulfen, Germany) with plastered ground and walls coated with Fluon® (Whitford GmbH, Diez, Germany) at 20°C and a 12h:12h light-dark cycle. Relative humidity inside these stock colonies ranged from 85.66 ± 3.61% RH to 99.69 ± 1.01% RH between the boxes. Honey, dead crickets and water (in Eppendorf cups with a cotton plug) were provided once a week *ad libitum*.

ACCLIMATION TREATMENTS

After keeping the colonies under lab conditions for at least two weeks (see above), we set up four temperature treatments: constant temperature at 12°C, 20°C and 28°C, respectively, and a fluctuating treatment with 12°C at night and 28°C during the day (with 3 h ramps between the two temperatures). For each of these treatments, we established two humidity conditions,

dry (~ 50% RH) and humid (~ 100% RH). From each of the ant colonies, we created eight worker groups, which were distributed among the eight treatments. They consisted of 6 foragers (collected outside the nest), 18 nurses (collected inside the nest, if possible directly from the brood) and 10 brood items. Foragers and nurses represent distinct behavioural castes in many ant species and are known to possess different CHC profiles (Greene and Gordon, 2003; Pamminger et al., 2014). We kept the worker groups in plastic boxes (95 x 95 x 60 mm, Westmark GmbH, Lennestadt-Elspe, Germany) with a plaster ground and a cavity (ca. 50 x 30 x 3 mm) covered with glass plates and red foil.

All climate treatments were established in climate cabinets (RUMED 3101 and 3201, Rubarth Apparate GmbH, Laatzen, Germany) equipped with two 1000-g air dehumidifiers ($CaCl_2$; UHU GmbH & Co. KG, Bühl/Baden, Germany) to keep the air in the cabinets as dry as possible. For the humid treatment, the boxes were covered with lids, while the lids for the dry treatment were prepared with a window closed with wire mesh (70 x 70 mm; mesh 0.2 mm) to ensure continuous airflow in the nest boxes. The worker groups were kept at the different acclimation treatments for three weeks. We provided food (honey and dead crickets) *ad libitum*. Water was provided in an Eppendorf cup (Eppendorf AG, Hamburg, Germany) with a piece of cotton. To maintain specific humidity levels, additional water was provided to the plaster in quantities adjusted to each treatment. Food and water were added depending on the temperature and humidity treatment: in 12°C *dry* only the Eppendorf cups were refilled every fourth day, in 20°C *dry* 1 ml of water was additionally applied on the plaster near the nest entrance every second day, while in the fluctuating temperature and 28°C *dry* treatments we similarly placed 1 or 2 ml (respectively) on the plaster. Humid kept ants were fed similarly and water added until the plaster was saturated with every feeding. Climatic conditions were surveyed using data loggers in additional, empty nest boxes (testo 174H, Testo AG, Lenzkirch, Germany), and we made sure that humidity levels were consistent

across temperature regimes (Table 1). After three weeks of acclimation, workers were taken for chemical analyses and survival tests.

CHEMICAL ANALYSES

We sampled two outside workers (foragers) and two inside workers (nurses) from each worker group (N = 480 per species). To correct for any potential daily fluctuations in CHC profile in the changing temperature treatments, we took one worker per caste at 8 am (end of the 12°C period) and the other one at 8 pm (end of the 28°C period). Each single worker was put into a glass vial and frozen at -20°C until the extraction.

We analyzed the cuticular hydrocarbons using gas chromatography – mass spectrometry (GC-MS). They were extracted by immersing single ants into *n*-hexane for ten minutes. During the extraction we added 100 ng *n*-octadecane (solved in 10 µl *n*-heptane) as internal standard for quantification of the absolute CHC amount. The extracts were transferred to a micro insert and concentrated under a gentle nitrogen stream to approximately 20 µl. Per sample, we then injected 2 µl into the GC (7890A, Agilent Technologies, Santa Clara, CA, USA) at a temperature of 250°C in splitless mode. As a carrier gas we used helium (He) with a flow rate of 1.2 ml per minute and a Zebron Inferno DB5-MS capillary column (length 30 m, Ø 0.25 mm, 0.25 µm coating, Phenomenex Ltd., Aschaffenburg, Germany) as stationary phase. The temperature program started at 60°C. After two minutes the oven heated with a rate of 60°C per minute up to 200°C and afterwards with a constant rate of 4°C per minute up to 320°C. This temperature was held constant for ten minutes. The analytes then entered the MS (5975C, Agilent Technologies) and were accelerated with an ionization voltage of 70 eV. The detector scanned for molecular fragments in a range of 40 – 550 m/z. Data was acquired using the software *MSD ChemStation* (E.02.02.1431; Agilent Technologies; Fig. 2). Hydrocarbons were identified based on retention index based on a standard series of *n*-

alkanes (Carlson et al., 1998) and diagnostic ions (Table A1). We excluded substances that were not hydrocarbons (< 10% of the total extract), substances with a maximum below 0.5 % and substances which occurred in less than 20 % of the samples of either species.

STATISTICAL ANALYSES: CHC PROFILES

We conducted all statistical analyses using *R* version 3.2.2 (R Core Team, 2017) and analyzed the following CHC traits: relative abundance of *n*-alkanes, mono-, di-, tri- and tetramethyl alkanes, alkenes, and alkadienes and the absolute CHC quantity. For each chemical trait and for both species separately, we constructed linear mixed-effects models (LME) (command *lme*, package *nlme*; Pinheiro et al., 2016), with temperature, humidity and caste as explanatory variables and colony ID and sampling location (nested in colony ID) as random effects. We reduced each model stepwise by removing the least significant interaction until AIC was minimal. If necessary, data was transformed and/or, in few cases, outliers were excluded (see Table 2A,B) to fulfil the model assumptions. Pairwise comparisons were executed using a Tukey test from the R package *lsmeans* (Lenth, 2016). In the results section, results for temperature, humidity and caste originated from the same models, but will be reported in separate chapters (see Table 2A,B). Here we focus on the CHC classes which were abundant and showed the strongest coefficient of variation in response to our experimental treatments, i.e. *n*-alkanes (*M. rubra*: $c_v = 0.615$; *M. ruginodis*: $c_v = 0.705$), dimethyl alkanes (*M. rubra*: $c_v = 0.306$; *M. ruginodis*: $c_v = 0.425$), alkenes (*M. rubra*: $c_v = 0.700$; *M. ruginodis*: $c_v = 0.438$) and alkadienes ($c_v = 0.349$, *M. ruginodis* only). Results for mono- (*M. rubra*: $c_v = 0.128$; *M. ruginodis*: $c_v = 0.237$), tri- and tetramethyl alkanes ($c_v = 0.490$ and $c_v = 0.358$, *M. rubra* only) are shown in Supplementary Fig. S1 and Supplementary Table S1. Methyl alkenes were not analyzed since their abundance was overall low (always < 2%) and zero in most cases.

Finally, we performed three comprehensive analyses to compare effect sizes between species and treatments, to assess overall CHC changes, and to analyze co-variation of substance classes. We compared overall CHC composition between climate regimes using PERMANOVA in the program PRIMER (Primer-E Ltd., Lutton, United Kingdom) with the same fixed and random factors as above, and visualized it using non-metric multidimensional scaling (NMDS) ordination. Hierarchical cluster analyses were performed (*hclust*, R package *vegan*; Oksanen et al., 2016) with the complete linkage method to determine which treatment groups were most similar to each other (Supplementary Fig. S2A,B). Co-variation among substance classes was analyzed using a principal component analysis (PCA) on the abundances of CHC classes (Supplementary Fig. S2C,D).

SURVIVAL EXPERIMENT

We placed one nurse and one forager from each of the constant temperature treatments (N = 360) in a polystyrole vial (Ø 28 mm, height 64 mm, volume 30 ml, K-TK e.K., Retzstadt, Germany) and plugged a piece of foam (1.04 ± 0.09 cm thick) in to about ⅓ of the height. We then filled it with 10.20 ± 0.96 g silica gel (2-5 mm, Sigma-Aldrich Laborchemikalien GmbH, Seelze, Germany) and sealed it airtight with Parafilm® (Bemis Flexible Packaging, Neetah, WI, USA). The silica gel was used to absorb the humidity within the vial (Bazinet et al., 2010; Stinziano et al., 2015). The experiment was performed in a climate chamber at 20°C. We checked survival first after six hours and afterwards once every hour until the 24th hour of the experiment. Ants that had died (defined here as the lack of any movement even after shaking the vial) in the first six hours (68 cases) were excluded from the data set since the exact time of death was uncertain. These 68 cases were distributed largely evenly across the treatments, with marginally more ants from the 28°C treatments (χ^2-test: $\chi^2_2 = 5.69$, $p = 0.058$). All observations were conducted blindly.

The data was analysed with a Cox mixed-effects model (command *coxme*; R package *coxme*; Therneau, 2015) comprising species, temperature, humidity and caste as explanatory variables. Colony ID and test day were implemented as random effects as this combination yielded the best AIC. Variables were tested with a type-II ANOVA (command *Anova*; package *car* version 2.1-1, adjusted by J. Fox 2015; Fox & Weisberg, 2011). We removed non-significant interactions stepwise until AIC was lowest.

MICRORHEOLOGY OF CUTICULAR HYDROCARBONS

To quantify the viscosity of CHC profiles, we used microrheology. This new approach allows measurements on small biological samples and cells, which were previously impossible due to the minute amounts of material available (for a review: Waigh, 2005). In passive microrheology (or particle tracking microrheology), the viscosity of a fluid is derived from the Brownian motion of microscopic probe particles embedded in the fluid. In complex fluids, microrheology also allows the investigation of viscoelastic properties and phase heterogeneity. Microrheology experiments are usually performed on small volumes of the order of 1 microlitre. We have developed a fluid collection procedure for micrometric droplets, allowing microrheology measurements on extremely small volumes of the order of 10 to 100 picolitres (Abou et al. 2010).

Particle-tracking microrheology experiments were performed on several extracts of *M. rubra* workers acclimated to constant, dry conditions at either 12°C or 28°C. The CHC extract of an ant worker was dissolved in 20 µl pentane and placed on a glass slide to evaporate the solvent. To collect the CHC extracts from the glass slide (on an inverted Leica DM IRB microscope, Leica Microsystems GmbH, Wetzlar, Germany), we used a fine glass micropipette connected to a pneumatic microinjector (CellTram Air, Eppendorf AG, Hamburg, Germany) mounted on a three-axis micro-manipulator (Burleigh, Thorlabs SAS,

293 Maisons-Laffitte, France). The fine tips (2-3 µm diameter) of the capillaries were prepared by
294 pulling from borosilicate glass micropipettes with 1 mm outer diameter and 0.78 mm inner
295 diameter (Harvard Apparatus S.A.R.L, Les Ulis Cedex, France) with a P-1000 Micropipette
296 puller (Sutter Instrument, Novato, CA, USA). The micropipette tip was moved onto the
297 surface in order to collect the largest possible amount of CHC extracts. Due to capillary
298 effects, the CHC extracts spontaneously rose in the micropipette as soon as the tip touched
299 the liquid.
300 Dry melamine beads (Acil, France; bead diameter: 0.740 ± 0.005 µm) were deposited on a
301 clean glass slide. The collected CHC extract was then ejected onto the beads by applying
302 positive pressure to the capillary via the microinjector. After ejection, the capillary tip was
303 moved along the glass slide to detach beads that were stuck to the glass surface. The CHC
304 fluid was then drawn up and ejected again several times in order to mix the beads with the
305 CHC extract (Abou et al., 2010).
306 The samples were observed using bright field microscopy at 100x magnification (oil
307 immersion objective, NA = 1.3, depth of focus: ~200 nm). The sample temperature was
308 controlled by adjusting the objective temperature with an objective heater (Bioptechs Inc.,
309 Butler, PA ,USA) to within ± 0.1 °C.
310 The Brownian motion of the tracer beads immersed in the CHC extract was recorded for 20 s
311 at 100 Hz with a fast sCMOS camera (OrcaFlash4.0 v2+, Hamamatsu Photonics France
312 S.A.R.L, Massy, France) mounted on the inverted microscope. For reliable analysis of the
313 Brownian motion, particular attention was paid to record only beads far from the surface of
314 the droplet or the glass slide. A self-written image analysis software allowed us to track the x
315 and y positions of any beads close to the focus plane of the objective. For each tracer bead,
316 the time-averaged mean squared displacement (MSD) was calculated as $< \Delta r^2(t) >_{t'} =$
317 $(\left(x(t'+t) - x(t')\right)^2 + (y(t'+t) - y(t')^2)_{t'}$. For Brownian motion of tracers in a

Newtonian fluid, the ensemble-averaged MSD increases linearly with the lag time, as $< \Delta r^2(t) >= 4Dt$ (in two dimensions), where D is the diffusion coefficient. In this case, the viscosity η can be estimated using the Stokes-Einstein relation, $\eta = {kT}/{6\pi RD}$, where R is the bead diameter and kT the thermal energy (Einstein, 1905).

We compared the viscosity of CHC extracts of *M. rubra* ants acclimated to 12°C and 28°C using a Wilcoxon rank sum test. Some samples were extremely viscous and could not be collected with micropipettes for measurement; these were assigned the highest viscosity ranks for statistical analysis. Further on, we tested whether the viscosity of a sample is linked to its chemical composition. Using Spearman's rank correlation, we tested whether viscosity was associated to the percentage of *n*-alkanes or dimethyl alkanes. These are the two substance classes that were both highly abundant and changed strongly during temperature acclimation.

Results

CHEMICAL ANALYSES

The climate treatments strongly affected the CHC profiles in both ant species (Fig. 3). Overall, temperature regime had by far the strongest impact on CHC composition (PERMANOVA, *M. rubra*: pseudo-F_3 = 69.5, *M. ruginodis*: pseudo-F_3 = 76.7, both p = 0.001; Supplementary Table S1). In contrast, humidity-induced effects were considerably smaller, especially so in *M. rubra* (*M. rubra*: pseudo-F_1 = 4.0, p = 0.007; *M. ruginodis*: pseudo-F_1 = 18.2, p = 0.001; Supplementary Table S1). Furthermore, nurses and foragers had strongly different profiles in both species (both pseudo-F_1 > 20.0; p = 0.001; Supplementary Table S1).

Effects of different constant temperatures

In spite of their strongly different CHC composition (Fig. 1, Fig. 2, Table A1), both *M. rubra* and *M. ruginodis* showed similar responses to the three *constant* temperature regimes: in both species, *n*-alkanes and alkenes increased with acclimation temperature. The increase was especially high between 20°C and 28°C, but weaker or, for alkenes in *M. ruginodis*, not detectable between 12°C and 20°C (Table 2A,B; Fig. 4A-D). Not only the relative amounts, but also the absolute quantities of *n*-alkanes increased with acclimation temperature (Supplementary Fig. S3). In contrast, dimethyl alkanes decreased with temperature, again with a particularly high shift between 20°C and 28°C in both species (Table 2A,B; Fig. 4E,F). Alkadienes, which were the dominant CHC class in *M. ruginodis* (34.68 ± 12.08%) but absent in *M. rubra*, similarly decreased at 28°C compared to 12°C or 20°C (Table 2B; Fig. 4G). Similar effects were found for tri-methyl alkanes, while the tetra-methyl alkanes showed opposite changes (both of which occurred in *M. rubra* only; Supplementary Table S1). Interestingly, monomethyl alkanes were the most abundant CHC class in *M. rubra* (48.39 ± 6.78%) and highly abundant in *M. ruginodis* (21.13 ± 5.00%), but showed only weak responses to climatic conditions (Supplementary Table S1, Supplementary Fig. S1).

Absolute CHC quantities decreased with acclimation temperature in *M. ruginodis*. In *M. rubra*, it was lowest at 28°C as well, but higher at intermediate temperatures than at 12°C (Table 2A,B; Supplementary Fig. S1A,B).

Constant vs. fluctuating temperature

Compared to constant temperatures, the fluctuating regime resulted in yet different CHC composition, and had different effects on the two ant species. In *Myrmica rubra*, profiles from fluctuating temperatures were relatively similar to those of 12°C and 20°C. In contrast, *M. ruginodis* profiles from the fluctuating treatment showed stronger differences two all three constant temperature regimes, but resembled more closely those of 28°C. This could be

confirmed for overall CHC composition with NMDS ordination (Fig. 3) and cluster analysis (Fig. S2A,B). Similar patterns were found for the percentages of substance classes: at fluctuating temperature, percentages of *n*-alkanes, dimethyl alkanes, and alkenes in *M. rubra* were similar to the 12°C treatment (Fig. 4A,C,E). In *M. ruginodis*, fluctuating temperatures led to alkene and dimethyl alkane percentages similar to the 28°C treatment, while *n*-alkanes and alkadienes were in between the 20°C and the 28°C treatments **(**Fig. 4D,F; Fig. 4B,G**)**. Absolute CHC quantities were highest at fluctuating temperatures in *M. rubra*, but had a low level comparable to the 28°C treatment in *M. ruginodis* (Supplementary Fig. S1A,B).

Effects of humidity

In both species, dry conditions led to a massive increase in absolute CHC quantity (Table 2A,B; Fig. 5A,B). However, CHC composition was less affected. In *M. rubra*, the only effect was an increase in alkenes under dry conditions. *Myrmica ruginodis* showed more changes under dry conditions, producing more alkenes (particularly in foragers) and less dimethyl alkanes (Table 2B, Supplementary Fig. S4D,F). Moreover, dry conditions led to an increase in *n*-alkanes at 28°C but not at 20°C or 12°C (Table 2B).

Differences between foragers and nurses

Foragers and nurses showed strong chemical differences, which were consistent across the two species (Supplementary Fig. S5). Foragers had more *n*-alkanes and alkenes, but less dimethyl alkanes (Table 2A,B; Supplementary Fig. S5A-F). Moreover, foragers had less alkadienes than nurses in *M. ruginodis*. In both species, nurses possessed more CHC (in µg) than foragers, except for dry-acclimated workers in *M. rubra* (interaction humidity x caste, Table 2A,B; Supplementary Fig. S5H,I). Contrary to our expectation, the two behavioural castes showed largely similar responses to the climatic treatments (i.e. no significant

interactions of caste with temperature or humidity), with few exceptions: forager-nurse differences in the percentage of *n*-alkanes in *M. ruginodis* (Table 2B) and alkenes in *M. rubra* (Table 2A) were only significant at 20°C and at fluctuating temperature (interaction temperature x caste). Foragers kept at dry conditions possessed more alkenes while they did not differ from nurses under humid conditions (interaction humidity x caste, Table 2B).

SURVIVAL EXPERIMENT

Ants of both species survived drought stress longer if they had acclimated to dry conditions compared to acclimation to humid conditions (Cox mixed-effects model: $\chi^2_1 = 33.07$, $p < 0.0001$; n = 292 ants; 40/292 still alive after 24h; Fig. 5C). Additionally, nurses survived better than foragers ($\chi^2_1 = 4.17$, $p = 0.041$). However, there was no difference between *M. rubra* and *M. ruginodis* workers ($\chi^2_1 = 0.16$, $p = 0.69$; Fig. 5C). Surprisingly, survival was neither influenced by the acclimation temperature ($\chi^2_2 = 1.50$, $p = 0.47$) nor any interaction of worker group, humidity and temperature (all non-significant after model reduction).

PHASE CHARACTERISTICS AND MICRORHEOLOGY OF CHC EXTRACTS

All CHC extracts were highly heterogeneous, with solid and liquid phases co-occurring even at ambient temperatures (Fig. 6A,B). Microrheology measurements on the liquid fraction of the CHC were conducted for *Myrmica rubra*. For several *M. rubra* colonies, extracts of cool-acclimated ants contained visible hydrocarbon crystals at temperatures below 20°C, which completely liquefied at T=25°C (Fig. 6C-F), suggesting a broad phase transition.

CHC viscosity was strongly correlated with the chemical composition of the CHC extracts. The viscosity increased with higher percentage of *n*-alkanes (Spearman's rank correlation: N = 17, $\rho = 0.65$, $p = 0.005$), but decreased with higher proportions of dimethyl-alkanes (N = 17, $\rho = -0.67$, $p = 0.003$). This suggests that warm-acclimated ants, due to their higher

amounts of *n*-alkanes and lower amounts of dimethyl alkanes, also should have more viscous CHC profiles. Indeed, extracts of ants acclimated to 28°C had a higher viscosity compared to those from 12°C-acclimated ants (Wilcoxon rank sum test: N = 17, W = 12, p = 0.027).

Fig. 7 shows one example of the measured mean squared displacement (MSD) of the tracers measured at 22°C for two extracts of ants from the same colony, one warm-acclimated and one cold-acclimated. Here, the extract from the 28°C-acclimated *M. rubra* was ca. 70 times as viscous as the one from the 12°C-acclimated worker of the same colony (7540±250 mPa·s vs. 110±5 mPa·s). The very large viscosity (~7000 times that of water) found in warm-acclimated *M. rubra* ants is consistent with the fact that four other extracts investigated were largely solid at 25°C, and too viscous to be collected with the micropipette (high *n*-alkanes contents up to 65%). These results suggest that the ants' acclimation to higher temperatures not only resulted in a higher proportion of CHC that were solid at ambient temperature, but also in a higher viscosity of the liquid CHC.

Discussion

Insects use a superficial layer of cuticular hydrocarbons for waterproofing their body (Hadley, 1994), and for a variety of other biological functions including, in particular communication (Blomquist and Bagnères, 2010; Leonhardt et al., 2016). The chemical composition of CHCs strongly influences these functions (Edney, 1977; Hadley, 1994), but the biophysical drivers of CHC variation are still poorly understood (Menzel et al., 2017). As insects have to survive under a variety of climatic conditions, the composition of their CHC layer may need to be adjusted to maintain its functions. This study is one of the first to disentangle the effects of humidity and temperature on cuticular hydrocarbon profiles, and to compare constant and fluctuating temperature regimes.

EFFECTS OF CONSTANT TEMPERATURE REGIMES

The different constant temperature regimes resulted in largely parallel changes in both species. After acclimation to higher temperatures, CHCs promoting tight molecular alignment (*n*-alkanes) increased in relative abundance, while substances disrupting molecular alignment (di- and trimethyl alkanes, alkadienes) decreased. Such changes have been reported previously to provide a better waterproofing of the cuticle (Gibbs and Mousseau, 1994; Menzel et al., 2018; Wagner et al., 2001). However, our data also show that acclimation to different temperatures did not have any effect on drought survival. This indicates that the observed temperature-induced changes of the CHC profile are not related to waterproofing. Although we cannot exclude that the changes are non-adaptive, e.g. due to shifts in physiological pathways, we hypothesise that they serve to adjust the viscosity of the CHC layer. A sufficiently low viscosity may be critical for maintaining many other functions essential biological functions of the CHC layer, including the transfer of communication cues, diffusion of recognition cues across the body surface, healing of scratches, lubrication and adhesion (Cooper et al., 2009; Dirks et al., 2010; Drechsler and Federle, 2006; Gorb, 2001; Wigglesworth, 1945). All these functions depend to some extent on the viscosity of the CHC layer. Generally, the viscosity of liquids increases when cooled to lower temperatures, until they solidify at the melting point. Consistent with the observed shift of the CHC composition towards compounds that disrupt molecular aggregation, acclimation to lower temperatures resulted in lower proportions (and lower absolute amounts) of *n*-alkanes, but higher proportions of dimethyl alkanes, which resulted in a reduced CHC viscosity. Clearly, these changes cannot be explained by waterproofing requirements, as tightly aggregating CHC could provide efficient waterproofing at both warm and cold temperatures. Instead, we hypothesise that a selection pressure could act to prevent complete CHC solidification at low

467 temperatures, because this would impede communication and other essential functions. One
468 mechanism to prevent solidification would be to maintain CHC viscosity at a constant low
469 level by adjusting the chemical composition of the CHC profile. A previous study on
470 membrane lipids in *Drosophila* reported comparable chemical changes during acclimation,
471 supporting the idea that acclimatory changes serve to maintain CHC viscosity (Overgaard et
472 al., 2006). Our data are consistent with a homeostatic control of viscosity. However, the
473 detailed adaptive benefits of low CHC viscosity have been largely ignored in previous work.
474 Future research should test whether low CHC viscosity is indeed maintained in a homeostatic
475 way, and study how changes in CHC composition and viscosity affect communication and
476 other functions. Our study shows that microrheology is a powerful method to address these
477 questions.
478 The strongest chemical changes, as measured by coefficients of variation, were found at the
479 opposite ends of the aggregative-disruptive gradient (*n*-alkanes, dimethyl alkanes,
480 alkadienes). Generally, higher concentrations (relative abundances) of *n*-alkanes (which
481 increase viscosity) coincided with lower concentrations of dimethyl alkanes, trimethyl
482 alkanes, methyl alkenes and alkadienes (all of which decrease viscosity). In contrast, only
483 weak acclimation effects were found for monomethyl alkanes, which may have intermediate
484 effects on viscosity, but were highly abundant in both species. This indicates that certain
485 CHC classes can vary relatively independently of each other (Supplementary Fig. S2C,D).
486 The different effect sizes show that it was mainly the most aggregating and the most
487 disruptive compounds that changed rather than the monomethyl alkanes. Surprisingly, the
488 relative abundance of alkenes increased with temperature, in parallel with the *n*-alkanes. The
489 significance of this finding is still unclear. Alkenes should reduce CHC viscosity and melting
490 points to a similar (or even higher) degree as dimethyl alkanes (Gibbs, 2002; Gibbs and
491 Pomonis, 1995). However, as alkenes and *n*-alkanes can crystallize separately (Gibbs, 2002),

a mixture of both might promote the persistence of liquid parts in the CHC layer even when *n*-alkanes are abundant.

A further unexpected result was that the absolute CHC quantity decreased with temperature. CHC quantities decreased in *M. ruginodis* from 12°C to 28°C, while in *M. rubra*, they were highest under fluctuating temperatures, but also lowest at 28°C. This result differs from previous studies where CHC quantity was unaffected by (Gibbs et al., 1998) or even increased with temperature (Gefen et al., 2015). A possible explanation for this pattern is that, at higher temperatures, cuticular hydrocarbons be lost faster via mechanical abrasion (when the ants are more active) or via footprints secreted from the tarsi during walking (Geiselhardt et al., 2010; Wüst and Menzel, 2017). However, our results show that the absolute amount of individual compounds such as *n*-alkanes increased at the highest temperatures, demonstrating that evaporation alone cannot explain the observed patterns.

EFFECTS OF FLUCTUATING TEMPERATURE

The difference between constant and fluctuating temperature regimes is crucial to understand how insects can cope with changing microclimate and weather conditions (Colinet et al., 2015). In many habitats, daily temperatures vary quickly, and probably faster than insects can acclimate. Interestingly, the CHC composition of ants from fluctuating regimes was not intermediate between the two corresponding constant temperatures: in *Myrmica rubra*, the fluctuating regime led to CHC profiles very similar to those of the coolest, constant regime. In contrast, the CHC profiles of *M. ruginodis* differed strongly from all constant temperature regimes (Fig. 3). Thus, temperature fluctuations had a stronger effect on *M. ruginodis* profiles than on *M. rubra* profiles, indicating that the two species differ in CHC changes during acclimation.

EFFECTS OF HUMIDITY

Both *Myrmica* species showed increased absolute CHC quantities under dry conditions. Similar increases were shown for scorpions (Gefen et al., 2015) and (albeit at high temperatures only) in desert beetles (Hadley, 1977). As expected, dry-acclimated individuals were more resistant to drought stress, consistent with previous studies, showing the adaptive value of this drought acclimation (Bazinet et al., 2010; Terblanche and Kleynhans, 2009). It is possible that reports of higher CHC quantities in insects acclimated to warm conditions are the result of stronger drought stress and not of the higher temperatures themselves (Hadley, 1977). In contrast to previous work, our experiments disentangled these two factors, and showed that higher temperatures even led to reduced overall CHC quantities once humidity was controlled for. Notably, temperature acclimation did not affect drought survival. Our results indicate that at least for *Myrmica*, CHC quantity is more important for desiccation resistance than CHC composition.

Drought stress may partly explain the differences between nurses and foragers: being more exposed to the sun, foragers may face higher desiccation stresses than nurses, consistent with their increase in *n*-alkane concentration and reduction in dimethyl alkanes. The smaller absolute quantity of CHCs in the foragers is surprising, as foraging workers may be more exposed to drought than nurses staying inside the relatively humid nest. In our opinion, the smaller CHC quantity in foragers is not adaptive but the result of higher CHC evaporation or abrasion during their outside activity (Johnson, 2000; Johnson and Gibbs, 2004), or of their higher age. This idea is corroborated by the lower desiccation survival of foragers than nurses in our assays.

MICRORHEOLOGY OF CUTICULAR HYDROCARBONS

All CHC extracts contained both solid and liquid fractions, at least at temperatures below 30°C. Early work established that water loss rates in insects are minimal at low temperatures, but increase suddenly once the temperature exceeds a 'critical' temperature (Ramsay, 1935; Wigglesworth, 1945). This sudden increase of water loss was shown in many insects to coincide with measured melting points of CHC extracts (Gibbs, 1998; Gibbs, 2002), suggesting that the increase in water permeability is explained by a melting of the lipid layer at this temperature. While CHC melting temperatures measured using capillary melting techniques, differential scanning calorimetry or infrared spectroscopy ranged from 27° to ca. 100°C (Gibbs, 2002), our observations show that liquid CHC are already present well below these temperatures, and that complex CHC profiles have a broad phase transition range rather than a single sharp melting point. This is evidenced by the observed coexistence of liquid and solid parts in CHC extracts. Moreover, the microrheology experiments show that even the liquid fraction itself is heterogeneous and exhibits locally varying viscosity.

Our microrheology measurements confirm that the ants' acclimation response modified the physical properties of the CHCs. The differences in viscosity can be explained by the observed changes in chemical composition: warm-acclimated ants showed higher amounts of solid *n*-alkanes and lower proportions of dimethyl alkanes, consistent with their more viscous CHC layers. Extracts from cold-acclimated ants had fewer *n*-alkanes, were less viscous and lacked any visible solid parts at 25°C measurement temperature. Our measurements show that the viscosity of CHC extracts provides a good proxy to assess lipid mobility on the cuticle surface, opening up avenues for future research.

Conclusions

Insect cuticular hydrocarbon profiles are astonishingly diverse. The different functions of CHC, particularly waterproofing and communication, depend on CHC composition and are

affected by temperature and humidity. CHC profiles are therefore linked to the insects' climatic niche, and their ability to acclimate or cope with short-term weather fluctuations. We have shown that, despite strong chemical differences, *Myrmica rubra* and *M. ruginodis* changed their profiles in similar and predictable ways during acclimation to constant temperatures (*n*-alkanes increased at higher temperatures, whereas dimethyl alkanes and alkadienes decreased) and humidity, and both species survived drought stress equally well. However, both species acclimated to fluctuating temperature regimes in a different way. While the profiles of *M. rubra* acclimated to fluctuating temperature was similar to those acclimated to constant 12°C or 20°C, profiles of *M. ruginodis* acclimated to fluctuating temperature differed from all constant temperature regimes. Both ant species responded to dry conditions by producing larger amounts of CHC, but only *M. ruginodis* also changed the composition of its profile. In sum, compared to *M. rubra*, *M. ruginodis* showed stronger CHC changes in response both to fluctuating temperature and drier conditions. Therefore, it is possible that CHC differences give rise to differences in position and width of microclimate niches, which may result in different microhabitats and geographic ranges.

CHC acclimation may be constrained by the need to maintain sufficiently low CHC viscosity for communication and other functions at low temperatures, and by the need to provide sufficient waterproofing at higher temperatures. In social insects in particular, CHC communication signals and recognition cues are exchanged between individuals. Future studies should investigate the biological effects of CHC viscosity and in particular address the effects of CHC acclimation on nestmate recognition and other functions. The trade-off between waterproofing and communication requirements makes the evolution and plasticity of CHC profiles an intriguing field of research with many open questions.

Acknowledgements

We thank Martin Woywod for his help in collecting the ant colonies and identifying the species. Furthermore, we thank Simone Glaser for help in data collection, as well as Heike Stypa, Steffi Emmling and Marion Kever for technical support of this study. Finally, we thank two anonymous reviewers for their comments which helped to improve this manuscript.

Competing interests

The authors declare no competing interests.

Author contributions

FM and PS conceived the study and developed the experimental setup. PS and LB performed the acclimation treatments and the chemical analyses. PS performed the survival tests. PS and FM performed the statistical analyses. BA and WF conducted the microrheological measurements. FM, PS, WF and BA wrote the manuscript. All authors approved the final version of the manuscript.

Funding

No funding has to be reported for this study.

Data Availability

All raw data will be published on Dryad upon acceptance of the manuscript.

References

Abou, B., Gay, C., Laurent, B., Cardoso, O., Voigt, D., Peisker, H. and Gorb, S. (2010). Extensive collection of femtolitre pad secretion droplets in the beetle *Leptinotarsa decemlineata* allows nanolitre microrheology. *J. R. Soc. Interface* **7**, 1745–1752.

Angilletta Jr., M. J. (2009). *Thermal Adaptation: A Theoretical and Empirical Synthesis*. Oxford, New York: Oxford University Press.

Bazinet, A. L., Marshall, K. E., MacMillan, H. A., Williams, C. M. and Sinclair, B. J. (2010). Rapid changes in desiccation resistance in *Drosophila melanogaster* are facilitated by changes in cuticular permeability. *J. Insect Physiol.* **56**, 2006–2012.

Beament, J. W. L. (1945). The cuticular lipoids of insects. *J. Exp. Biol.* **21**, 115–131.

Beament, J. W. L. (1958). The Effect of Temperature on the Water-proofing Mechanism of an Insect. *J. Exp. Biol.* **35**, 494–519.

Beament, J. W. L. (1959). The Waterproofing Mechanism of Arthropods I. The Effect of Temperature on Cuticle Permeability in Terrestrial Insects and Ticks. *J. Exp. Biol.* **36**, 391–422.

Blomquist, G. J. (2010). Structure and analysis of insect hydrocarbons. In *Insect Hydrocarbons: Biology, Biochemistry, and Chemical Ecology* (ed. Blomquist, G. J.) and Bagnères, A.-G.), pp. 19–34. New York: Cambridge University Press.

Blomquist, G. J. and Bagnères, A.-G. (2010). Introduction: history and overview of insect hydrocarbons. In *Insect Hydrocarbons: Biology, Biochemistry, and Chemical Ecology* (ed. Blomquist, G. J.) and Bagnères, A.-G.), pp. 3–18. New York: Cambridge University Press.

Brooks, L., Brunelli, M., Pattison, P., Jones, G. R. and Fitch, A. (2015). Crystal structures

of eight mono-methyl alkanes (C26–C32) via single-crystal and powder diffraction and DFT-D optimization. *IUCrJ* **2**, 490–497.

Carlson, D. A., Bernier, U. R. and Sutton, B. D. (1998). Elution patterns from capillary GC for methyl-branched alkanes. *J. Chem. Ecol.* **24**, 1845–1865.

Chown, S. L., Sørensen, J. G. and Terblanche, J. S. (2011). Water loss in insects: an environmental change perspective. *J. Insect Physiol.* **57**, 1070–1084.

Colinet, H., Sinclair, B. J., Vernon, P. and Renault, D. (2015). Insects in fluctuating thermal environments. *Annu. Rev. Entomol.* **60**, 123–140.

Cooper, R., Lee, H., González, J. M., Butler, J., Vinson, S. B. and Liang, H. (2009). Lubrication and Surface Properties of Roach Cuticle. *J. Tribol.* **131**, 14502.

Coumou, D. and Rahmstorf, S. (2012). A decade of weather extremes. *Nat. Clim. Chang.* **2**, 491–496.

Dirks, J.-H., Clemente, C. J. and Federle, W. (2010). Insect tricks: two-phasic foot pad secretion prevents slipping. *J. R. Soc. Interface* **7**, 587–593.

Drechsler, P. and Federle, W. (2006). Biomechanics of smooth adhesive pads in insects: Influence of tarsal secretion on attachment performance. *J. Comp. Physiol. A* **192**, 1213–1222.

Edney, E. B. (1977). *Water Balance in Land Arthropods*. Berlin, Heidelberg, New York: Springer.

Einstein, A. (1905). Über die von der molekularkinetischen Theorie der Wärme geforderte Bewegung von in ruhenden Flüssigkeiten suspendierten Teilchen. *Ann. Phys.* **18**, 549–560.

Fischer, K., Kölzow, N., Höltje, H. and Karl, I. (2011). Assay conditions in laboratory experiments: Is the use of constant rather than fluctuating temperatures justified when investigating temperature-induced plasticity? *Oecologia* **166**, 23–33.

Fox, J. and Weisberg, S. (2011). An R Companion to Applied Regression.

Fung, F., Lopez, A. and New, M. (2011). Water availability in +2°C and +4°C worlds. *Philos. Trans. R. Soc. A* **369**, 99–116.

Gefen, E., Talal, S., Brendzel, O., Dror, A. and Fishman, A. (2015). Variation in quantity and composition of cuticular hydrocarbons in the scorpion *Buthus occitanus* (Buthidae) in response to acute exposure to desiccation stress. *Comp. Biochem. Physiol. Part A* **182**, 58–63.

Geiselhardt, S. F., Lamm, S., Gack, C. and Peschke, K. (2010). Interaction of liquid epicuticular hydrocarbons and tarsal adhesive secretion in *Leptinotarsa decemlineata* Say (Coleoptera: Chrysomelidae). *J. Comp. Physiol. A* **196**, 369–378.

Gibbs, A. G. (1995). Physical properties of insect cuticular hydrocarbons: model mixtures and lipid interactions. *Comp. Biochem. Physiol.* **112B**, 667–672.

Gibbs, A. G. (1998). The Role of Lipid Physical Properties in Lipid Barriers. *Am. Zool.* **38**, 268–279.

Gibbs, A. G. (2002). Lipid melting and cuticular permeability: new insights into an old problem. *J. Insect Physiol.* **48**, 391–400.

Gibbs, A. G. and Mousseau, T. A. (1994). Thermal Acclimation and Genetic Variation in Cuticular Lipids of the Lesser Migratory Grasshopper (*Melanoplus sanguinipes*): Effects of Lipid Composition on Biophysical Properties. *Physiol. Zool.* **67**, 1523–1543.

Gibbs, A. G. and Pomonis, J. G. (1995). Physical properties of insect cuticular

hydrocarbons: The effects of chain length, methyl-branching and unsaturation. *Comp. Biochem. Physiol.* **112B**, 243–249.

Gibbs, A. G., Louie, A. and Ayala, J. (1998). Effects of temperature on cuticular lipids and water balance in a desert Drosophila: is thermal acclimation beneficial? *J. Exp. Biol.* **80**, 71–80.

Gorb, S. (2001). *Attachment devices of insect cuticle*. Dordrecht, Boston: Kluwer Academic Publishers.

Greene, M. J. and Gordon, D. M. (2003). Cuticular hydrocarbons inform task decisions. *Nature* **423**, 32.

Hadley, N. F. (1977). Epicuticular lipids of the desert Tenebrionid beetle, *Eleodes armata*: Seasonal and acclimatory effects on composition. *Insect Biochem.* **7**, 277–283.

Hadley, N. F. (1994). *Water Relations of Terrestrial Arthropods*. San Diego: Academic Press.

Johnson, R. A. (2000). Water loss in desert ants: caste variation and the effect of cuticle abrasion. *Physiol. Entomol.* **25**, 48–53.

Johnson, R. A. and Gibbs, A. G. (2004). Effect of mating stage on water balance, cuticular hydrocarbons and metabolism in the desert harvester ant, *Pogonomyrmex barbatus*. *J. Insect Physiol.* **50**, 943–953.

Labonte, D. and Federle, W. (2015). Rate-dependence of “wet” biological adhesives and the function of the pad secretion in insects. *Soft Matter* **11**, 8661–8673.

Lenth, R. V (2016). Least-Squares Means: The R Package lsmeans. *J. Stat. Softw.* **69**, 1–33.

Leonhardt, S. D., Menzel, F., Nehring, V. and Schmitt, T. (2016). Ecology and evolution

of communication in social insects. *Cell* **164**, 1277–1287.

Maitani, M. M., Allara, D. L., Park, K. C., Lee, S. G. and Baker, T. C. (2010). Moth olfactory trichoid sensilla exhibit nanoscale-level heterogeneity in surface lipid properties. *Arthropod Struct. Dev.* **39**, 1–16.

Menzel, F., Blaimer, B. B. and Schmitt, T. (2017). How do cuticular hydrocarbons evolve? Physiological constraints and climatic and biotic selection pressures act on a complex functional trait. *Proc. R. Soc. B* **284**, 20161727.

Menzel, F., Zumbusch, M. and Feldmeyer, B. (2018). How ants acclimate: Impact of climatic conditions on the cuticular hydrocarbon profile. *Funct. Ecol.* **32**, 657–666.

Oksanen, J., Blanchet, F. G., Friendly, M., Kindt, R., Legendre, P., McGlinn, D., Minchin, P. R., O'Hara, R. B., Simpson, G. L., Solymos, P., et al. (2016). vegan: Community Ecology Package.

Overgaard, J., Sørensen, J. G., Petersen, S. O., Loeschcke, V. and Holmstrup, M. (2006). Reorganization of membrane lipids during fast and slow cold hardening in *Drosophila melanogaster*. *Physiol. Entomol.* **31**, 328–335.

Pamminger, T., Foitzik, S., Kaufmann, K. C., Schützler, N. and Menzel, F. (2014). Worker Personality and Its Association with Spatially Structured Division of Labor. *PLoS One* **9**, e79616.

Pinheiro, J., Bates, D., DebRoy, S., Sarkar, D. and R Core Team (2016). nlme: Linear and Nonlinear Mixed Effects Models.

R Core Team (2017). R: A Language and Environment for Statistical Computing.

Radchenko, A. G. and Elmes, G. W. (2010). Myrmica *ants (Hymenoptera: Formicidae) of the old world*. Warsaw: Natura optima dux Foundation.

Ramsay, J. A. (1935). The evaporation of water from the cockroach. *J. Exp. Biol.* **12**, 373–383.

Rourke, B. C. and Gibbs, A. G. (1999). Effects of lipid phase transitions on cuticular permeability: Model membrane an in situ studies. *J. Exp. Biol.* **202**, 3255–3262.

Seebacher, F., White, C. R. and Franklin, C. E. (2015). Physiological plasticity increases resilience of ectothermic animals to climate change. *Nat. Clim. Chang.* **5**, 61–66.

Stinziano, J. R., Sové, R. J., Rundle, H. D. and Sinclair, B. J. (2015). Rapid desiccation hardening changes the cuticular hydrocarbon profile of *Drosophila melanogaster*. *Comp. Biochem. Physiol. Part A* **180**, 38–42.

Terblanche, J. S. and Kleynhans, E. (2009). Phenotypic plasticity of desiccation resistance in *Glossina* puparia: are there ecotype constraints on acclimation responses? *J. Evol. Biol.* **22**, 1636–1648.

Therneau, T. M. (2015). coxme: Mixed Effects Cox Models.

van Dooremalen, C., Suring, W. and Ellers, J. (2011). Fatty acid composition and extreme temperature tolerance following exposure to fluctuating temperatures in a soil arthropod. *J. Insect Physiol.* **57**, 1267–1273.

Wagner, D., Tissot, M. and Gordon, D. (2001). Task-related environment alters the cuticular hydrocarbon composition of harvester ants. *J. Chem. Ecol.* **27**, 1805–1819.

Waigh, T. A. (2005). Microrheology of complex fluids. *Reports Prog. Phys.* **68**, 685–742.

Wigglesworth, V. B. (1945). Transpiration through the cuticle of insects. *J. Exp. Biol.* **21**, 97–114.

Wüst, M. and Menzel, F. (2017). I smell where you walked - how chemical cues influence

movement decisions in ants. *Oikos* **126**, 149–160.

Tables

Table 1. Mean temperature and humidity of the treatments. Shown is the mean ± standard deviation of temperature [°C] and relative humidity [% RH].

Temperature	**dry**	**humid**
12°C	12.42 ± 0.39°C	12.50 ± 0.40°C
	61.84 ± 9.95% RH	99.72 ± 1.03% RH
20°C	19.66 ± 0.15°C	19.99 ± 0.18°C
	49.58 ± 8.28% RH	99.97 ± 0.97% RH
28°C	26.72 ± 0.32°C	27.27 ± 0.41°C
	50.99 ± 12.88% RH	99.78 ± 0.79% RH
fluctuating	19.25 ± 7.23 °C	19.58 ± 7.31 °C
temperature	58.79 ± 12.43% RH	99.74 ± 0.79% RH

Table 2. Model results for chemical traits of A) *M. rubra* and B) *M. ruginodis*. All results from linear mixed effects models (LME) including colony ID and sampling location as random factors. Superscript letters denote whether data were a) log-, b) logit-, c) arcsine-square root- transformed, d) not transformed. In some cases outliers were removed to fulfil model assumptions (see N). All dependent variables except for absolute quantity are relative abundances.

A) *M. rubra*

Dependent variable	Fixed effect	N	df	χ^2	p
***n*-alkanes** [b]	Temperature	480	3	200.51	< 0.0001
	Humidity		1	1.65	0.19
	Caste		1	27.03	< 0.0001
dimethyl alkanes [d]	Temperature	476	3	197.54	< 0.0001
	Humidity		1	1.84	0.17
	Caste		1	52.94	< 0.0001
alkenes [c]	Temperature	473	3	240.80	< 0.0001
	Humidity		1	14.67	0.0001
	Caste		1	45.41	< 0.0001
	Temperature x Caste		3	11.04	0.011
absolute quantity [a]	Temperature	472	3	199.33	< 0.0001
	Humidity		1	106.36	< 0.0001
	Caste		1	3.88	0.049

B) *M. ruginodis*

***n*-alkanes** [b]	Temperature	480	3	388.21	< 0.0001
	Humidity		1	8.88	0.0029
	Caste		1	51.28	< 0.0001
	Temp. x Humidity		3	14.02	0.0029
	Temperature x Caste		3	9.60	0.022
dimethyl alkanes [d]	Temperature	480	3	253.49	< 0.0001
	Humidity		1	19.89	< 0.0001
	Caste		1	42.00	< 0.0001
alkenes [b]	Temperature	480	3	208.71	< 0.0001
	Humidity		1	31.40	< 0.0001
	Caste		1	22.02	< 0.0001
	Humidity x Caste		1	3.97	0.046
alkadienes [d]	Temperature	480	3	172.97	< 0.0001
	Humidity		1	2.66	0.10
	Caste		1	38.91	< 0.0001
absolute quantity [a]	Temperature	473	3	35.24	< 0.0001
	Humidity		1	50.11	< 0.0001
	Caste		1	17.33	< 0.0001
	Humidity x Caste		1	6.64	0.010

Table A1. Cuticular hydrocarbon profiles of *M. rubra* and *M. ruginodis*. Overall, we detected and identified 64 hydrocarbon peaks in *M. rubra* and 69 peaks in *M. ruginodis*. The table shows the retention index (Kovats index; RI) (Carlson et al., 1998), substance name, diagnostic ions (mass peaks are printed in italics) and its mean percentage ± SD. Double bond positions for most abundant substances were determined by DMDS derivatisation (see diagnostic ions in brackets). Tentative identifications are marked by asterisks.

				M. rubra	***M. ruginodis***
#	**RI**	**Substance**	**Diagnostic ions (m/z)**	**Mean ± SD**	**Mean ± SD**
1	19.01	n-C19	*268*	0.29 ± 0.27	0.51 ± 0.68
2	19.59	unknown CHC	-	0.16 ± 0.13	-
3	23.02	n-C23	*324*	0.28 ± 0.37	-
4	23.53	5-MeC23	85/281	0.13 ± 0.12	-
5	24.02	n-C24	*338*	0.29 ± 0.19	0.05 ± 0.12
6	24.77	C25-ene	*350*	0.06 ± 0.1	-
7	24.96	C25-ene	*350*	1.1 ± 0.92	-
8	25.03	n-C25	*352*	5.51 ± 4.41	0.12 ± 0.16
9	25.36	9-;11-;13-MeC25	140/252; 168/224; 196	1.7 ± 0.75	-
10	25.43	7-MeC25	112/280	1.5 ± 0.97	-
11	25.52	5-MeC25	84/308	1.41 ± 0.8	-
12	25.67	8,12-DiMeC25	126/280, 196/210	0.47 ± 0.24	-
13	25.74	3-MeC25	56/336	1.26 ± 0.61	-
14	25.84	5,9-;5,11-DiMeC25	85/323, 154/252, 182/224	0.74 ± 0.41	-
15	26.01	n-C26	*366*	0.61 ± 0.26	0.05 ± 0.07
16	26.11	3,x-DiMeC25	56/364	0.37 ± 0.16	-
17	26.36	10-MeC26*	154/252	0.47 ± 0.39	-
18	26.4	8-MeC26*	126/280	0.82 ± 0.56	-
19	26.64	10,14-DiMeC26	154/266, 224/196	0.34 ± 0.3	-
20	26.68	8,12-DiMeC26	126/294, 196/224	0.5 ± 2.04	-
21	26.77	6,10-; 6.12-DiMeC26	98/322, 168/252 196/224	0.34 ± 0.24	-
22	26.98	C27-ene	*378*	1.83 ± 1.56	-
23	27.01	n-C27	*380*	3.37 ± 1.98	2.72 ± 2.26
24	27.2	4,8,12-TriMeC26	70/378, 140/308, 210/238	0.32 ± 0.33	-
25	27.34	11-;13-MeC27	168/252; 196/224	-	0.18 ± 0.15
26	27.36	9-;11-MeC27	140/280; 168/252	15.47 ± 4.89	-
27	27.43	7-MeC27	112/308	2.18 ± 1.58	0.21 ± 0.27
28	27.53	5-MeC27	85/337	4.93 ± 2.2	0.21 ± 0.23
29	27.63	11,15-DiMeC27	168/266, 238/196	5.39 ± 2.47	-
30	27.66	9,13-DiMeC27	140/294, 210/224	-	0.02 ± 0.05
31	27.72	7,11-DiMeC27	112/323, 183/252	8.15 ± 3.77	-
32	27.74	3-MeC27	57/365	0.15 ± 0.54	0.44 ± 0.49
33	27.84	5,11-DiMeC27	85/351, 183/253	5.23 ± 2.35	-

34	27.98	7,11,15-TriMeC27	112/337, 183/267, 253/197	1.35 ± 1.32	-
35	28.01	7,11,21-TriMeC27	112/337, 183/267, 337/112	0.68 ± 0.56	-
36	28.01	n-C28	*394*	-	0.33 ± 0.32
37	28.1	5,9,13-;5,9,15-TriMeC27	85/364, 154/294, 225, 253/197	1.6 ± 0.59	-
38	28.35	7-;10-;12-;13-;14-MeC28	112/323; 155/281; 181/253; 197/238; 210/225	1.87 ± 0.78	-
39	28.38	3,7,11-TriMeC27	56/392, 126/322, 196/252	0.33 ± 0.5	-
40	28.46	unknown CHC	-	0.12 ± 0.11	-
41	28.64	3,7,11,15-TetraMeC27	57/407, 127/337, 197/267, 267/197	1.8 ± 0.67	-
42	28.64	C29diene	*404*	-	0.42 ± 0.61
43	28.68	C29diene	*404*	-	0.92 ± 0.74
44	28.73	C29ene	*406*	-	1.23 ± 0.56
45	28.76	3,x,y,z-TetraMeC27	56/406	0.36 ± 0.29	-
46	28.79	C29-9-ene	*406*, [173, 327, 500]	-	4.18 ± 1.52
47	28.86	C29-7-ene	*406*, [145, 355, 500]	-	2.29 ± 1.1
48	28.9	C29ene	*406*	-	0.5 ± 0.42
49	29.01	n-C29	*408*	1.62 ± 1.12	5.22 ± 4.25
50	29.18	4,8,16-TriMeC28 (position of 3rd methyl group tentative)	71/393, 141/323, 267/196	0.04 ± 0.08	-
51	29.24	x-MeC29-diene	-	-	0.3 ± 0.24
52	29.33	9-;11-;13-;15-MeC29	141/308; 167/281; 197/252; 224	8.32 ± 2.85	7 ± 2
53	29.42	7-MeC29	112/336	1.06 ± 0.64	0.16 ± 0.44
54	29.52	5-MeC29	84/364	1.83 ± 0.97	1.5 ± 0.9
55	29.6	11,15-;13,17-DiMeC29	168/295, 239/224; 196/267, 267/196	3.27 ± 1.56	0.68 ± 0.81
56	29.7	9,13-; 7,11-DiMeC29	140/322, 210/252; 112/350, 182/280	-	0.49 ± 0.74
57	29.74	3-MeC29	57/393	2.51 ± 0.86	2.24 ± 0.85
58	29.82	5,17-DiMeC29	85/379, 267/196	2.64 ± 0.93	0.63 ± 0.37
59	29.87	5-21-DiMeC29*	85/379, 323/140	0.05 ± 0.11	-
60	29.98	7,11,17-TriMeC29	112/364, 183/296, 281/196	0.29 ± 0.31	-
61	30.05	n-C30	*422*	-	0.21 ± 0.21
62	30.07	3,11*-DiMeC29	56/406, 182/280	0.53 ± 0.37	-
63	30.31	10-;12-;13-;14-MeC30	154/308; 182/280; 196/266; 210/252	0.46 ± 0.25	0.59 ± 0.31
64	30.36	unknown CHC	-	0.12 ± 0.14	-
65	30.49	C31diene	*432*	-	0.11 ± 0.14
66	30.55	C31diene	*432*	-	0.42 ± 0.53
67	30.65	C31diene	*432*	-	4.76 ± 1.94
68	30.65	2-;4-MeC30	43/420; 71/393	0.62 ± 0.5	-
69	30.7	C31diene	*432*	-	14.35 ± 6.61
70	30.7	C31-11-ene	*434*, [201, 327, 528]	-	2.44 ± 3.61
71	30.8	C31diene	*432*	-	1.67 ± 2.54
72	30.8	C31-9-ene	*434*, [173, 355, 528]	-	8.63 ± 5.28
73	30.87	C31ene	*434*	-	0.68 ± 0.98
74	30.91	C31ene	*434*	-	0.92 ± 0.77

75	31	n-C31	*436*	-	0.46 ± 0.63
76	31.16	unknown CHC	-	-	0.32 ± 0.39
77	31.21	13-;14-MeC31ene	*448*, 194/278, 210/266	-	1.51 ± 0.82
78	31.3	9-;11-;13-;15-MeC31	140/336; 168/308; 196/280; 224/252	-	6.33 ± 2.37
79	31.32	13-;15-MeC31	196/280; 224/252	1.35 ± 0.94	-
80	31.41	7-MeC31	112/364	0.19 ± 0.18	-
81	31.44	cf. Methyltrien (unknown unsaturated)	-	-	0.42 ± 0.45
82	31.52	5-MeC31	85/392	0.04 ± 0.12	-
83	31.56	13,17-DiMeC31	196/295, 267/224	0.98 ± 0.81	3.46 ± 2.49
84	31.62	13,21-DiMeC31*	196/294, 322/168	0.07 ± 0.12	-
85	31.65	9,17-;9,19-;9,21-DiMeC31	140/350, 266/224, 294/196, 322/168	-	2.48 ± 2.17
86	31.7	unknown CHC	-	0.13 ± 0.15	-
87	31.74	3-MeC31	57/420	-	0.83 ± 0.67
88	31.8	5,15-;5,17-DiMeC31	85/407, 239/252, 267/224	0.19 ± 0.14	1.08 ± 0.64
89	32.04	3,15-DiMeC31	57/435, 239/252	-	0.3 ± 0.28
90	32.3	12-;13-;14-;15-;16-MeC32	182/308; 196/294; 210/280; 224/267; 238/252	0.04 ± 0.08	0.22 ± 0.22
91	32.51	C33diene	*460*	-	0.54 ± 0.52
92	32.57	C33diene	*460*	-	1.78 ± 0.98
93	32.65	C33diene	*460*	-	4.63 ± 1.89
94	32.73	C33diene	*460*	-	1.46 ± 1.14
95	32.79	C33diene	*460*	-	0.87 ± 1.11
96	32.87	C33ene	*462*	-	0.14 ± 0.2
97	33.13	unknown CHC	-	-	0.1 ± 0.16
98	33.3	11-;13-;15-;17-MeC33	169/336; 196/309; 224/280; 252	0.07 ± 0.16	1.11 ± 0.89
99	33.46	unknown CHC	-	0.05 ± 0.13	-
100	33.54	13,17-;13,19-DiMeC33	196/323, 267/252, 295/224	-	0.62 ± 0.59
101	33.61	9,x-;11,x-DiMeC33 [x=17 or 19]	140/379, 168/350, 267/252, 294/224	-	0.59 ± 0.6
102	33.67	unknown CHC	-	-	0.05 ± 0.11
103	33.78	5,21-;5,23-DiMeC33	84/434, 322/196, 350/168	-	0.43 ± 0.35
104	34.04	3,15-DiMeC33	56/462, 238/280	-	0.12 ± 0.24
105	34.45	C35diene	*488*	-	0.31 ± 0.39
106	34.49	C35diene	*488*	-	0.34 ± 0.38
107	34.55	C35diene	*488*	-	1.33 ± 1.06
108	34.65	C35diene	*488*	-	0.22 ± 0.35
109	35.24	13-;15-;17-MeC35	196/336; 224/338; 252/280	-	0.09 ± 0.18
110	35.4	15,x-DiMeC35	224/322	0.02 ± 0.07	-
111	35.45	15,19-DiMeC35	224/322, 294/252	-	0.23 ± 0.37
112	35.51	11/13/15/17,19/21/23-DiMeC35 (combination of methyl group positions unknown)	168/378, 196/350, 224/322, 252/294, 294/252, 322/224, 350/196	-	0.12 ± 0.16
113	36.41	C37diene	*516*	-	0.13 ± 0.22

Figure legends

Fig. 1. Composition of CHC profiles according to substance classes ordered by chain length for (A) *M. rubra* and (B) *M. ruginodis*. Plotted is the mean relative abundance of substance classes ordered by chain length from C19 to C37. As shown here, the CHCs of each species are confined to a small range of chain lengths only. Beside differences in CHC classes (visualised by colour codes), *M. ruginodis* has longer hydrocarbons than *M. rubra*, the most common chain length being C31 vs. C27, respectively. Relations between CHC composition and chain length have been found across a wide range of species and may relate to their viscosity (Menzel et al. 2017). For the sake of clarity, we did not separate different CHCs of the same chain length and substance class. For detailed composition see Table A1.

Fig. 2. Representative profiles of (A) *M. rubra* and (B) *M. ruginodis*. Each peak represents one substance (or mixture which could not be separated by gas chromatography). Numbers refer to the substances listed in Table A1. Note that we show only retention times with relevant peaks (i.e. minute 10-25 for *M. rubra* and minute 15-30 for *M. ruginodis*).

Fig. 3. Non-metric multidimensional scaling (NMDS) ordinations of the chemical profiles of (A) *M. rubra* and (B) *M. ruginodis*, calculated for two dimensions. The ellipses show the 95% confidence areas around the centroids for each climate regime (temperature: 12°C, 20°C, 28°C and fluc – fluctuating; humidity: d – dry and h – humid). Each dot represents one sample (note that some dots lie outside of the plotted range).

Fig. 4. Effects of treatment temperature on the ants' CHC profiles. The upper row shows *M. rubra*, the bottom row *M. ruginodis*. The plots visualize the effects of four different temperature treatments (12°C, 20°C, 28°C and fluctuating, each represented by similar colour

code as in Fig. 2 for easier comparison) on the proportions of *n*-alkanes (A,B), dimethyl alkanes (C,D), alkenes (E,F) and alkadienes (G). All graphs show back-transformed means ± SE. Different letters indicate statistically significant differences according to pairwise Tukey-tests on the LME data ($p < 0.05$).

Fig. 5. Effects of humidity on the ants' absolute CHC amount and survival. (A) and (B) show the absolute amount of CHCs [µg] of *M. rubra* and *M. ruginodis* workers acclimated to humid and dry conditions (back-transformed means of log-transformed data ± SE). Significant differences are indicated by asterisks, *** $p < 0.001$. (C) Worker survival of dry conditions over time. The Kaplan Meier plot shows that the two species do not differ in survival, but that there is an effect of acclimation to dry vs. humid conditions on survival rate.

Fig. 6. Solid and liquid phases of CHC extracts of *M. rubra*. The CHC extract from a 28°C-acclimated ant (A) contains much more solid phase compared to the mixture of solid and liquid phases in CHC extracts of a 12°C-acclimated ant (B) (photos taken at 25°C). The photos in (C-F) show transmitted (C, E) and crossed-polarized light (D, F) photos of CHC extracts from *M. rubra* ants acclimated to 12°C. Solid crystals are visible at 18.4°C (C, D) but not at 25°C (E, F), indicating a broad transition range and the existence of solid and liquid phases at ambient temperatures.

Fig. 7. Microrheology of CHC in *M. rubra* ants. The plot shows the time-averaged mean-squared displacement (MSD) of 0.74µm-diameter melamine tracer beads undergoing Brownian motion within the CHC sample. *M. rubra* ants acclimated to 28°C (bottom) had CHC that exhibited lower MSD (indicating a higher CHC viscosity) than ants acclimated to 12°C (top).

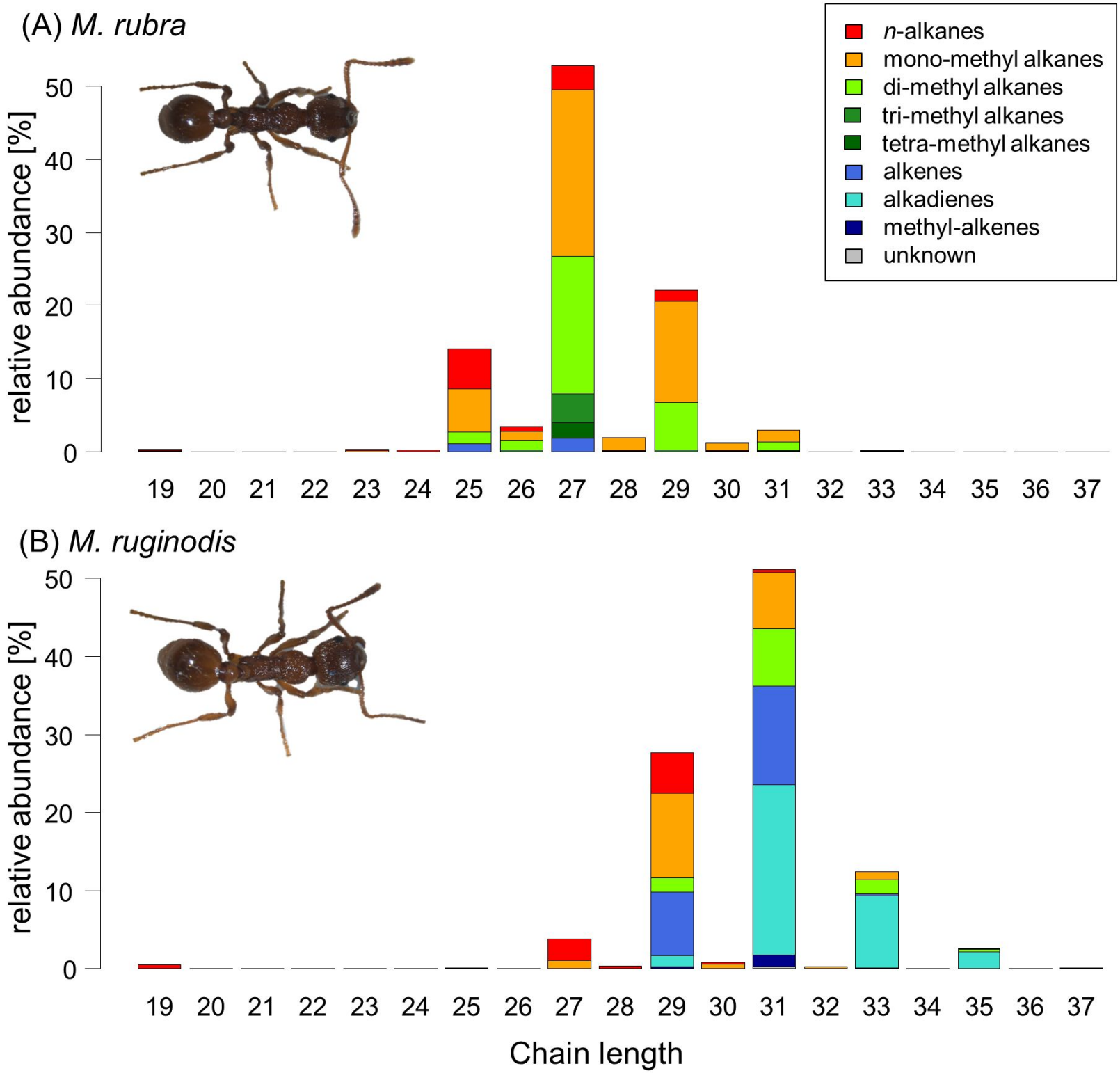
(A) M. rubra
(B) M. ruginodis
n-alkanes
mono-methyl alkanes
di-methyl alkanes
tri-methyl alkanes
tetra-methyl alkanes
alkenes
alkadienes
methyl-alkenes
unknown
relative abundance [%]
0
10
20
30
40
50
19 20 21 22 23 24 25 26 27 28 29 30 31 32 33 34 35 36 37
Chain length

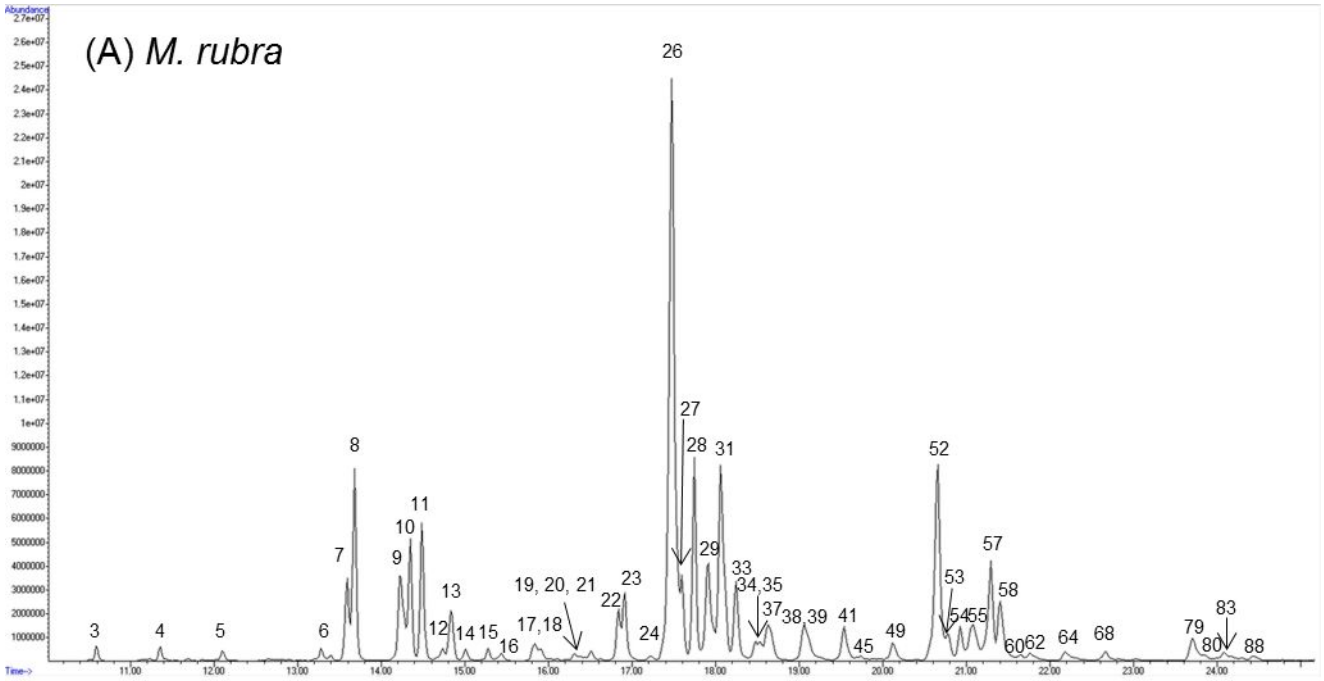
(A) M. rubra
Abundance
Time-->
3
4
5
6
7
8
9
10
11
12
13
14
15
16
17,18
19, 20, 21
22
23
24
26
27
28
29
31
33
34,35
37
38,39
41
45
49
52
53
54
55
57
58
60
62
64
68
79
80
83
88

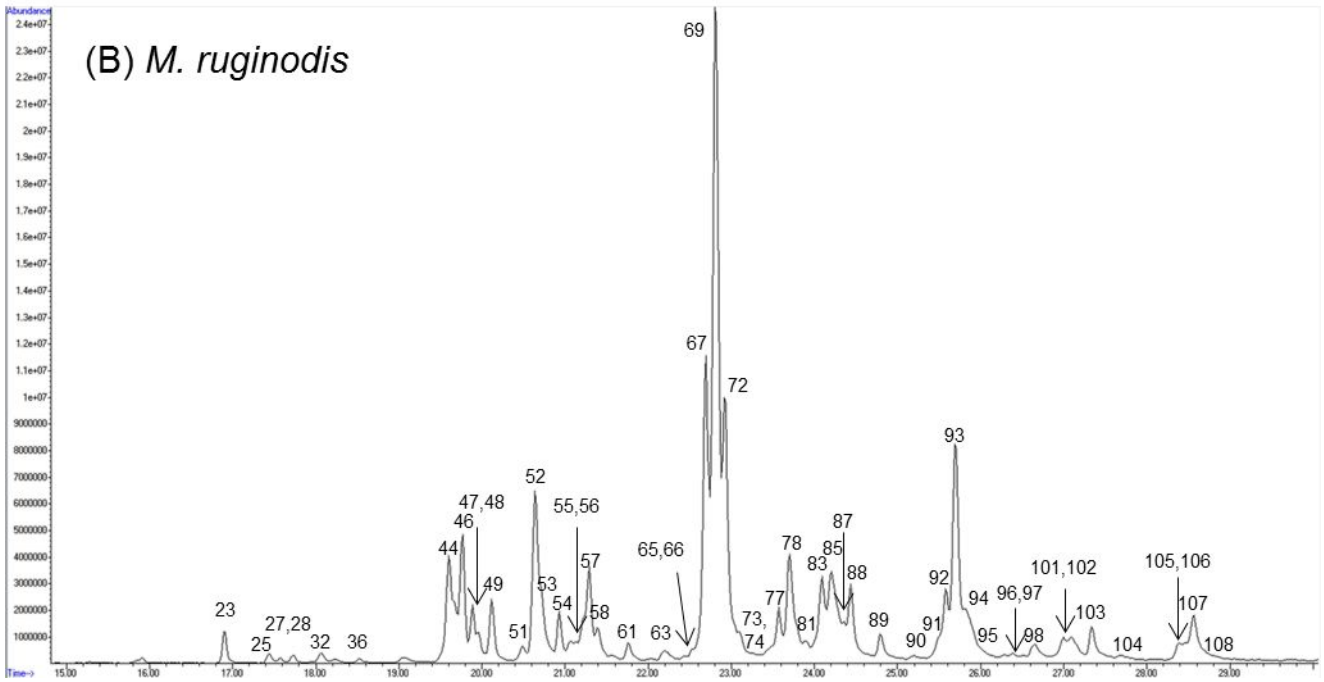
(B) M. ruginodis
Abundance
Time-->
23
25
27,28
32
36
44
46
47,48
49
51
52
53
54
55,56
57
58
61
63
65,66
67
69
72
73,
74
77
78
81
83
85
87
88
89
90
91
92
93
94
95
96,97
98
101,102
103
104
105,106
107
108

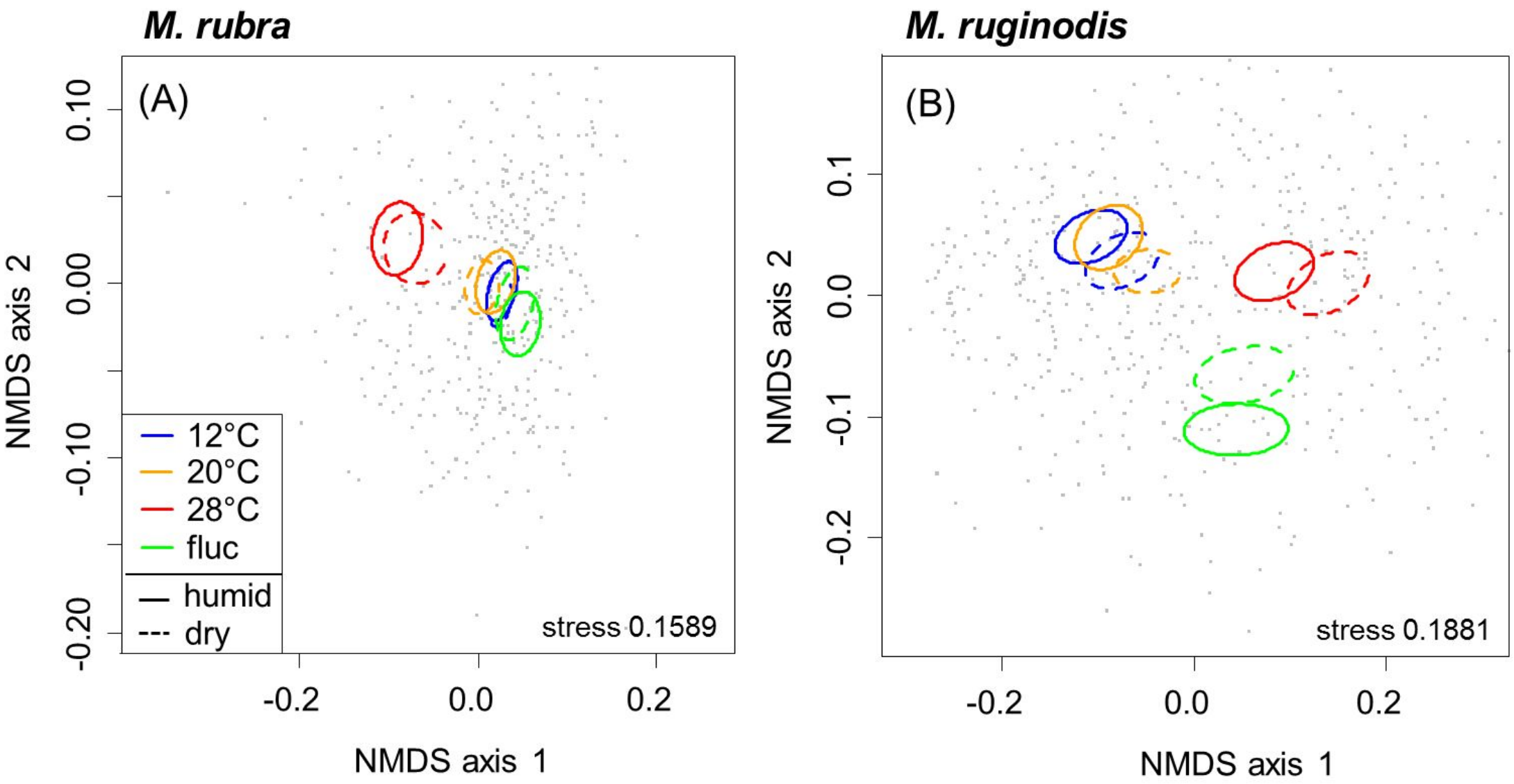
M. rubra
(A)
NMDS axis 2
0.10
0.00
-0.10
-0.20
-0.2
0.0
0.2
NMDS axis 1
12°C
20°C
28°C
fluc
humid
dry
stress 0.1589
M. ruginodis
(B)
NMDS axis 2
0.1
0.0
-0.1
-0.2
-0.2
0.0
0.2
NMDS axis 1
stress 0.1881

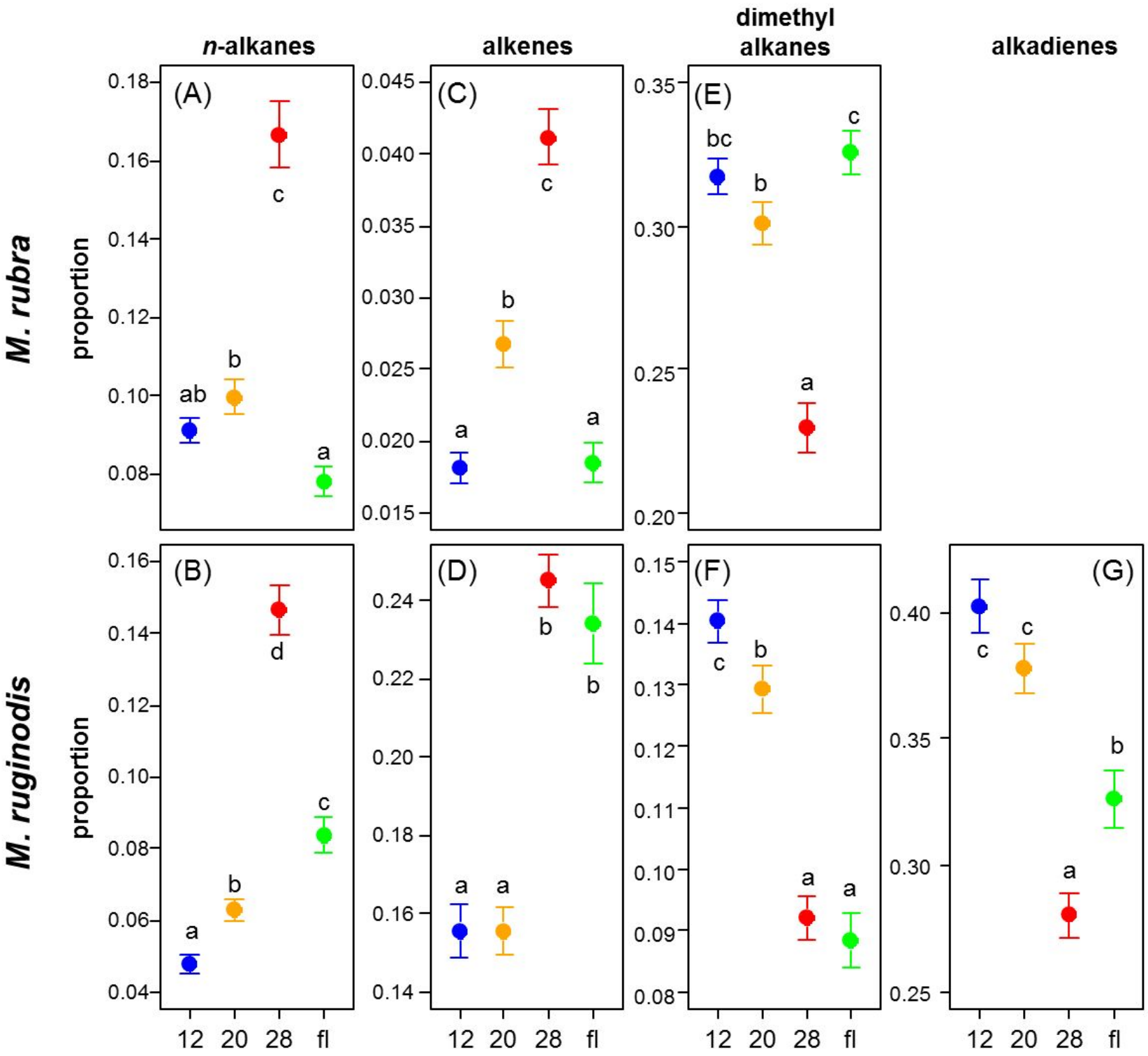
n-alkanes
alkenes
dimethyl alkanes
alkadienes
M. rubra
M. ruginodis
proportion
(A)
(B)
(C)
(D)
(E)
(F)
(G)
12
20
28
fl

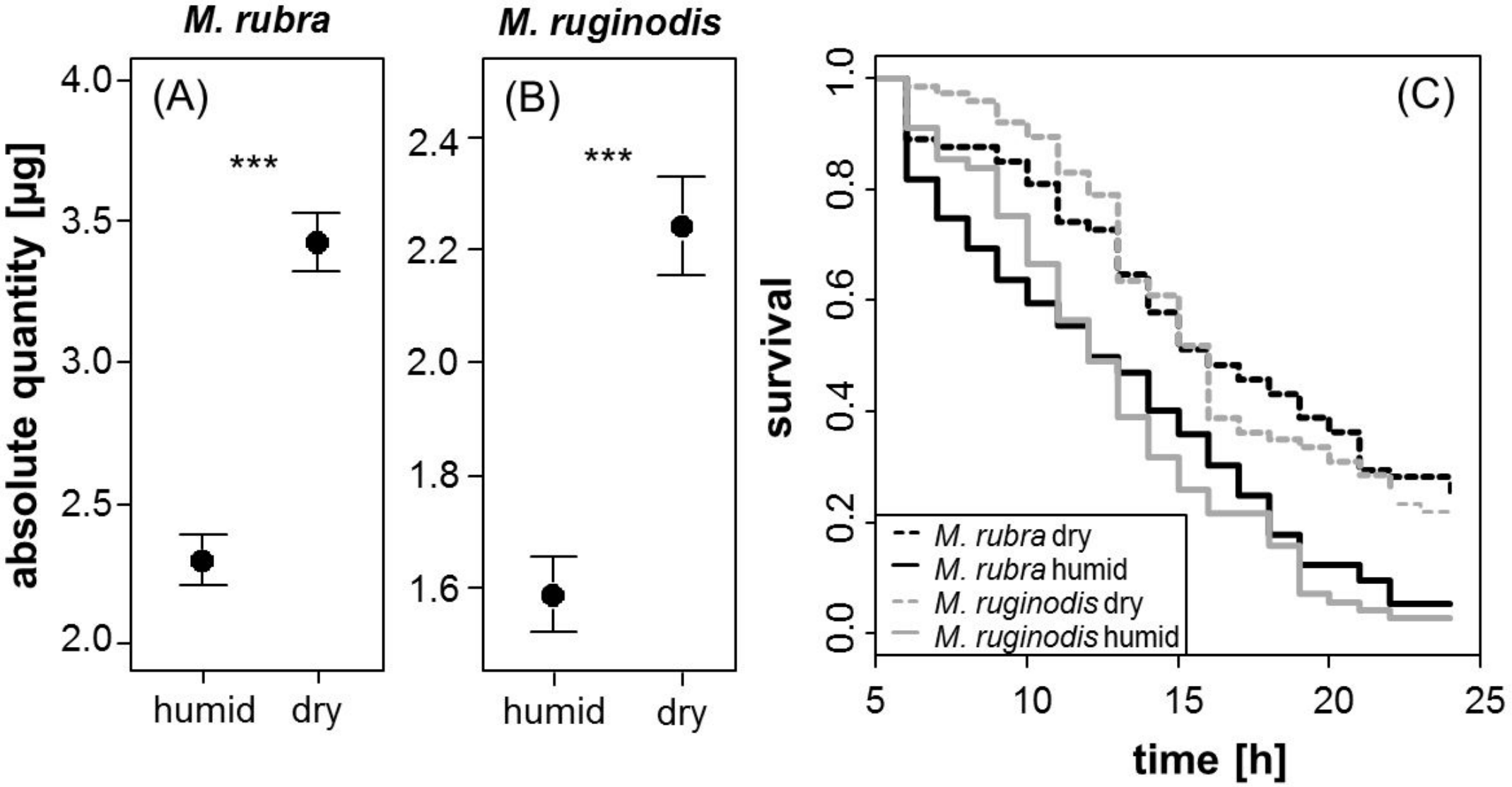
M. rubra
M. ruginodis
(A)
(B)
(C)
***
***
absolute quantity [µg]
4.0
3.5
3.0
2.5
2.0
2.4
2.2
2.0
1.8
1.6
humid
dry
humid
dry
survival
1.0
0.8
0.6
0.4
0.2
0.0
5
10
15
20
25
time [h]
M. rubra dry
M. rubra humid
M. ruginodis dry
M. ruginodis humid

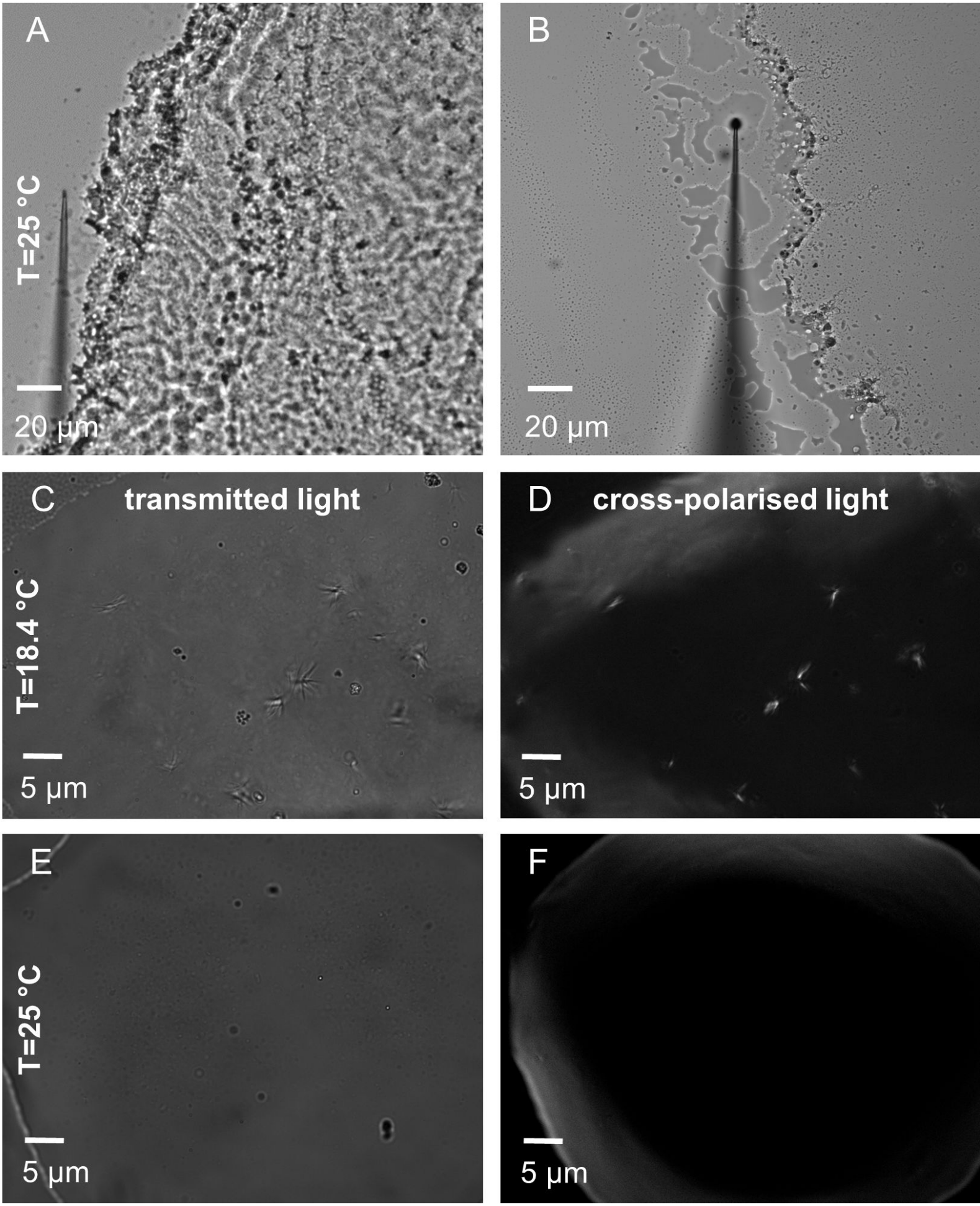
A
T=25 °C
20 µm
B
20 µm
C
transmitted light
T=18.4 °C
5 µm
D
cross-polarised light
5 µm
E
T=25 °C
5 µm
F
5 µm

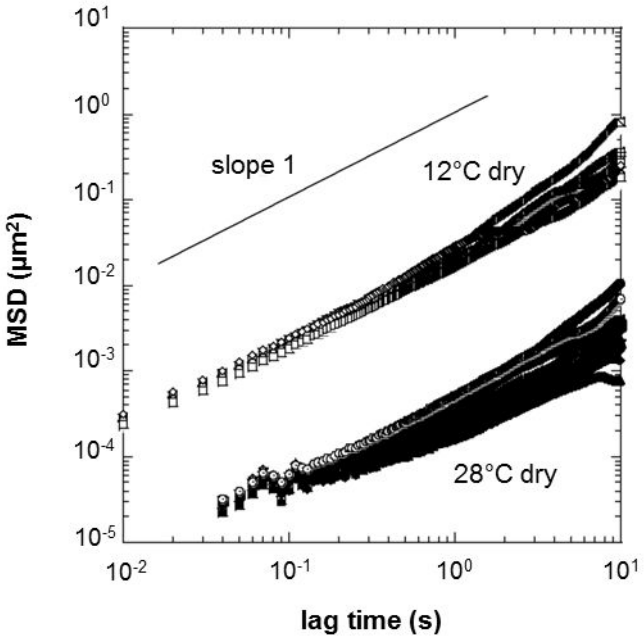
MSD (μm²)
lag time (s)
slope 1
12°C dry
28°C dry
10¹
10⁰
10⁻¹
10⁻²
10⁻³
10⁻⁴
10⁻⁵
10⁻²
10⁻¹
10⁰
10¹